Quaternary Science Advances 13 (2024) 100133

Contents lists available at ScienceDirect

Quaternary Science Advances

journal homepage: www.sciencedirect.com/journal/quaternary-science-advances

# A multi-proxy reconstruction of the late Holocene vegetation dynamics in Krabi mangroves, Thailand Andaman Sea

Paramita Punwong [a,b,*], Apichaya Englong [c], Rob Marchant [b], Akkaneewut Jirapinyakul [d], Ausanee Suttiwong [a], Prae Chirawatkul [e], Ponlachart Chotikarn [f,g], Nathsuda Pumijumnong [a], Monthira Yuttithum [a], Pasin Maprasop [h], Waratthaya Promchoo [h]

[a] Faculty of Environment and Resource Studies, Mahidol University, Phutthamonthon Sai 4 Road, Nakhon Pathom, 73170, Thailand
[b] York Institute of Tropical Ecosystems, Department of Environment and Geography, University of York, York, YO10 5NG, UK
[c] Biological Sciences Program, Department of Botany, Faculty of Science, Chulalongkorn University, Patumwan, Bangkok, 10330, Thailand
[d] Center of Excellence for the Morphology of Earth Surface and Advanced Geohazards in Southeast Asia (MESA CE), Department of Geology, Faculty of Science, Chulalongkorn University, Patumwan, Bangkok, 10330, Thailand
[e] Synchrotron Light Research Institute (Public Organization), 111 University Avenue, Muang District, Nakhon Ratchasima, 30000, Thailand
[f] Marine and Coastal Resources Institute, Faculty of Environmental Management, Prince of Songkla University, Hat Yai, Songkhla, 90110, Thailand
[g] Coastal Oceanography and Climate Change Research Center, Prince of Songkla University, Hat Yai, Songkhla, 90110, Thailand
[h] Mangrove Research and Development Institute, Department of Marine and Coastal Resources, Ministry of Natural Resource and Environment, 120 Ratthaprasasanaphakdi Building, Chaengwattana Road, Thung Song Hong, Lak Si, Bangkok, 10210, Thailand

ARTICLE INFO

*Keywords:*
Pollen analysis
Charcoal analysis
Sea-level changes
Coastal changes
Malay-Thai peninsula

ABSTRACT

Pollen, charcoal, loss on ignition, geochemistry, and geophysical analyses were used to reveal the palaeoenvironment, vegetation, and sedimentary dynamics of the Krabi mangroves and the Andaman coast during the late Holocene. Two sediment cores, radiocarbon dated to ~4400 cal BP, were collected from the Nai Nang mangroves in Krabi Province, the Thailand Andaman coast. This analysis documented how the area evolved from a tidal channel to a tidal area dominated by mangrove ecosystems. During the tidal channel phase (~4400–2700 cal yr BP), the study site was characterized by a high-energy depositional environment, where sediment accumulated along tidal channels. Mangrove development began around 4400 cal yr BP and was influenced by varying contributions from tidal and freshwater inputs. Sea level during this period showed a slight rise until ~4200 cal yr BP, followed by a subsequent fall. From ~2700 to 1050 cal yr BP, the tidal channel was filled with finer sediments, forming intertidal flats that supported mangroves, back mangroves, and freshwater forest taxa, indicating a transition to mixed coastal vegetation. Sea levels remained relatively low during this period. From around 1050 cal yr BP to the present, mangroves replaced the previous mixed coastal vegetation, most likely driven by rising sea levels, particularly during the last 200 years. The observed sedimentation rates indicate that mangroves in Krabi will need to undergo continued future landward migration to adapt to changing coastal conditions, given the current and projected global sea-level rise.

## 1. Introduction

Sea-level changes have been the main factors influencing coastal configuration and ecosystem dynamics on the Thailand Andaman coast along the Malay-Thai Peninsula (Tjia, 1996; Scoffin and Tissier, 1998; Scheffers et al., 2012; Oliver and Terry, 2019). The Malay-Thai Peninsula is tectonically stable and remote from isostatic ice-loading effects (Tjia, 1996; Woodroffe and Horton, 2005). Previous investigations of Holocene relative sea level (RSL) using geophysical data from fringing reefs and oysters have consistently documented sea-level transgression during the early Holocene (Tjia, 1996; Scoffin and Tissier, 1998; Scheffers et al., 2012; Oliver and Terry, 2019). Some studies also revealed that a mid-Holocene highstand occurred during the mid-Holocene (between 5700 and 5000 yr cal BP), which was approximately 2.5–5 m above the present mean sea level, before eventually declining to the present level (Scoffin and Tissier, 1998; Oliver and Terry, 2019; Scheffers et al., 2012). More widely, sea-level studies on the west coast of Malaysia and Singapore have shown highstands from

* Corresponding author. Faculty of Environment and Resource Studies, Mahidol University, Phutthamonthon Sai 4 Road, Nakhon Pathom, 73170, Thailand.
*E-mail address:* paramita.pun@mahidol.edu (P. Punwong).

https://doi.org/10.1016/j.qsa.2023.100133
Received 7 August 2023; Received in revised form 7 October 2023; Accepted 10 October 2023
Available online 11 October 2023
2666-0334/© 2023 The Authors. Published by Elsevier Ltd. This is an open access article under the CC BY-NC-ND license (http://creativecommons.org/licenses/by-nc-nd/4.0/).

~5100 to 4000 cal yr BP (Mann et al., 2019; Chua et al., 2021). These studies were consistent with the ICE-6G GIA model, indicating a mid-Holocene highstand at ~6500 cal yr BP and a gradual decline in the RSL during the late Holocene (Peltier et al., 2015). However, some studies have indicated that sea level fluctuated after the mid-Holocene highstand before reaching the present level (Tjia, 1996; Fujimoto et al., 1999; Scheffers et al., 2012). Tjia (1996) proposed a mid-Holocene highstand at approximately 6000 cal yr BP along with additional highstand events at approximately 4000 and 2700 cal yr BP. Fujimoto et al. (1999) suggested that sea level rose from 7200 years BP and reached a maximum level of 1 m above the present mean sea level around 6100 years BP. Subsequently, sea level fluctuated until 2200 cal yr BP, followed by a gradual rise to the present level. However, a recent investigation into sea-level change within the Andaman Sea recorded a consistent trend of rising sea level between 1972 and 2011 with a high variation of +1.4–6.7 mm year$^{-1}$ (Putcharapitchakon and Ritphring, 2012).

Mangroves are unique ecosystems found in tropical coastal regions between the terrestrial and marine environments. These ecosystems consist of evergreen trees and shrubs that have adapted to growing in physiologically challenging intertidal zones (Hogarth, 2015). Mangroves can withstand a range of salinity levels, ranging from fully marine water in the lowest intertidal areas to freshwater in upstream rivers, depending on the flood tide gradient and freshwater runoff (Wang and Gu, 2021). This adaptability is due to their unique physiology enable allowing them to survive the highly dynamic and challenging conditions in the intertidal zone (Krauss et al., 2008; Hogart, 19992015; Krauss et al., 2008).

Mangroves are vulnerable to multiple factors such as regional climate changes, fluctuations in relative sea level (RSL), and anthropogenic activities (Punwong et al., 2012, 2018, 2023) that often combine to increase the impact on the coastal zone. Sediments accumulated within mangrove ecosystems are an important source of information for understanding past vegetation changes and RSL fluctuations, serving as sensitive sea-level indicators (Woodroffe, 2009; Punwong et al., 2012, 2013a, 2013b). Numerous studies have used fluctuations in mangrove pollen composition and distribution within sediment cores to reconstruct and understand historical sea-level fluctuations (Woodroffe, 2009; Punwong et al., 2012, 2013a, 2013b, 2018, 2023; Moraes et al., 2017; Ribeiro et al., 2018; Englong et al., 2019, 2023). In addition to RSL fluctuations, mangrove ecosystem composition can also be influenced by factors such as rainfall and human interaction (Gilman et al., 2008; Wang and Gu, 2021). Variations in rainfall patterns play a crucial role in determining freshwater runoff, sediment flow, and nutrient influx into mangroves, ultimately affecting salinity and overall ecosystem composition. Charcoal is a valuable palaeoecological indicator for understanding fire history, resulting from either natural fires, human activities, or a combination of both (Whitlock and Larsen, 2001). In conjunction with pollen analysis, charcoal is commonly employed to explore the intricate relationships between ecosystems, climate change, fires, and human activities. Moreover, the size of charcoal particles can provide insights into the proximity of fire sources, helping to differentiate between regional and local fire occurrences (Clark and Royall, 1995; Whitlock and Larsen, 2001) that can be used for climatic interpretation, such as changing rainfall regimes (Githumbi, 2017; Punwong et al., 2023). Mangrove dynamics are also influenced by other factors, such as the depositional environment (Moraes et al., 2017; Ribeiro et al., 2018). Although the Andaman coast supports most of Thailand's mangrove forests, mangrove dynamics and their response to RSL oscillations remain poorly understood. Through the analysis of stratigraphic profiles, pollen, charcoal, and geochemical signatures, this study developed a model to describe the evolution of mangrove dynamics and their responses to climate and sea-level changes, as well as local depositional environments in Nai Nang, Krabi Province, Thailand (Fig. 1).

### 1.1. Site descriptions

#### 1.1.1. General setting

Nai Nang is located on the western coast of the Malay-Thai Peninsula in Khoa Khram District, Krabi Province, and is traversed by the tidal channels (Fig. 1). Mangroves at Nai Nang covers approximately 10 km$^2$ and are under the influence of semi-diurnal tidal patterns with a range of 1.4–2.8 m at Ao Nang (Admiralty Tide Tables, 2014). The region is also affected by tidal channels that carry freshwater from terrestrial sources during the rainy season, leading to seasonal variations in salinity. Elevated areas are used for agriculture, such as rubber and palm plantations, and orchards by local communities (Land Development Department, 2020).

#### 1.1.2. Climate and mangrove vegetation

The western coast of the Malay-Thai Peninsula is characterised by a tropical monsoonal climate. The southwest monsoon transports humid air masses from the Indian Ocean, increasing the rainfall from mid-May to October. The northeast monsoon starts in mid-November and precipitation decreases between November and April. The intense solar radiation, reversal of monsoons, and high humidity increase

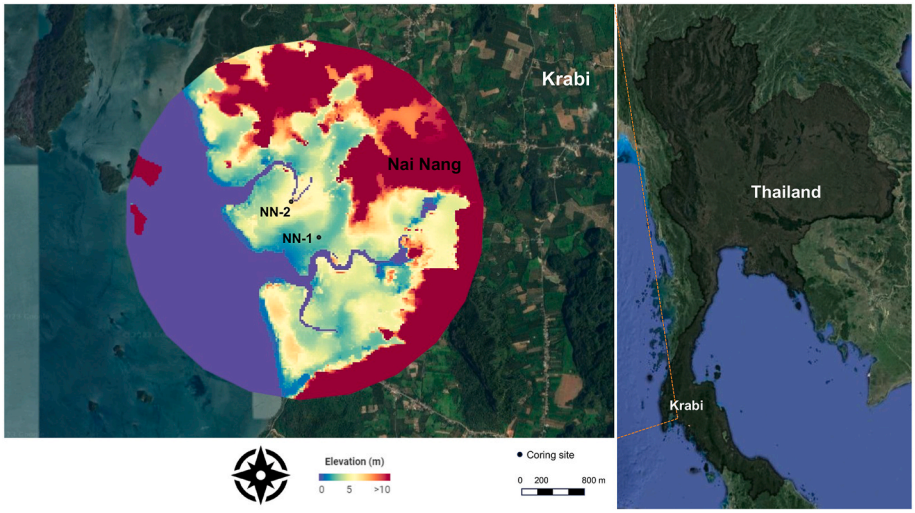


**Fig. 1.** Map showing the study area and the estimation of elevation relying on the utilization of a novel dataset known as the Forest and Buildings (FABDEM) of Nai Nang and coring sites (NN-1 and NN-2).

temperature from February to April. The annual mean temperature in the region is approximately 27 °C, with temperatures ranging from 22 °C to 39 °C. On average, the annual mean precipitation is approximately 2100 mm year$^{-1}$ (Climate Center, 2023).

Mangrove vegetation has been classified into two types, namely 'true mangroves' and 'back mangroves' based on their degree of saltwater inundation (Watson, 1928; Santisuk, 1983). True mangroves occur in areas inundated by high tides, including seaward zones, whereas back mangroves are restricted to areas that are occasionally inundated by the sea, particularly during very high tides. In Krabi, true mangrove taxon namely *Rhizophora apiculata* is the dominant mangrove species followed by *Ceriops tagal* and back mangrove species; *Xylocarpus granatum* and *X. moluccensis*. Other true mangrove taxa, such as *R. mucronata*, *Bruguiera cylindrica*, *B. gymnorrhiza*, and *Avicennia officinalis*, have also been found (Department of Marine and Coastal Resources, 2018).

## 2. Methodology

Two sediment cores; NN-1 (2.35 m depth, 8°12′28.0″N/98°45′26.4″E) and NN-2 (3.30 m depth, 8°12′47.5″N/98°45′12.0″E) were collected in 2022 from the mangrove areas close to Nai Nang village, Krabi province (Fig. 1) with a 50-cm long 5 cm diameter Russian corer. The cores were taken from two boreholes with a 10 cm overlap between each 50 cm core drive. The core samples were placed in PVC pipes, wrapped in plastic sheets, and transported before storage at 4 °C. Ecosystem surveys to record plant species at each site and vegetation in 10 m$^2$ nested quadrats were set up over the coring site to establish the plant composition surrounding each coring site.

Sediment characteristics were described based on a modified version of the Tröels-Smith classification (Kershaw, 1997). The sedimentary sequences were subsampled at intervals of 10 cm along the entire length of each core for further palaeoecological analyses, including pollen, charcoal, loss on ignition, stratigraphy, particle size, and geochemical analyses set within the radiocarbon chronology. Sediment samples (1 cm$^3$) were used to determine pollen concentrations using the acetolysis method (Faegri and Iversen, 1989). Pollen grains in the extracted samples were identified by comparison with pollen obtained from present-day specimens and modern pollen references (Chumchim, 2010). *Bruguiera* and *Ceriops* were grouped together as *Bruguiera/Ceriops* because of their similar pollen morphologies under a light microscope (Grindrod, 1985). A minimum of 300 grains were counted for each sample and categorised according to ecological habitat as mangroves, back mangroves, terrestrial herbaceous, non-mangrove arboreal (lowland forest), and unknown. The classification of mangroves and back mangroves is based on inundation classes (Santisuk, 1983). Terrestrial pteridophyte spores and algae were excluded from the pollen sums. Pollen data are presented as pollen percentage diagrams and zoned using stratigraphically constrained cluster analysis (CONISS) (Grimm, 1991). Pollen-slide charcoal analysis was conducted to reconstruct the fire history using the size class of microscopic charcoal modified from Rucina et al. (2010). Total charcoal accumulation was calculated following the method described by Punwong et al. (2018).

To determine the grain-size distribution, the samples were pretreated with 30% $H_2O_2$ to eliminate organic matter, followed by 10% HCl to remove carbonates. The prepared samples were eventually analysed by laser diffraction using a Malvern Mastersizer 2000 analyser, range of 0.02–2000 μm. The sub-samples were dried and weighed for loss on ignition at 550 °C and 950 °C based on Heiri et al. (2001) for carbon and carbonate measurements, respectively. X-ray fluorescence (XRF) was used for geochemical analysis of a set of elements, including Ti, Cu, Zn, Pb, Fe, K, Ca, Mn, and Ni for each subsample. The analysis was performed at the Synchrotron Light Research Institute, Nakhon Ratchasima, using a 19-element Ge detector. PyMCA (Solé et al., 2007) was used to calculate the results, following the method outlined by Punwong et al. (2023). Seven pre-treated sediment samples, identified from depths of notable biostratigraphic change and the basal depths of each core, were selected for AMS dating and submitted to the DirectAMS Radiocarbon Dating Service, USA. The dating results were calibrated with the northern hemisphere calibration of the Intcal20 curve (Reimer et al., 2020) at 2σ-confidence using OxCal v4.4.4 (Bronk-Ramsey, 2021). The highest relative probability of calibration was selected to construct the age model for linear interpolation between the adjacent dated samples. This model allowed us to approximate the ages of the pollen zones. All palaeoecological data were plotted as diagrams using the graphics software TILIA2 and TILIA*Graph (Grimm, 1991). Principal component analysis (PCA) was performed using SPSS version 28 to gain insight into the relationship between the palynological, sediment, and geochemical compositions. Estimation of elevation relies on the utilization of a novel dataset known as FABDEM (Forest and Buildings removed Copernicus DEM) (Hawker et al., 2022; Uhe et al., 2022). FABDEM is the first 30m global digital elevation model (DEM) dataset that effectively eliminates the presence of trees and buildings using machine learning correction.

## 3. Results

The integration of stratigraphy, particle size, pollen, charcoal and geochemical records allowed us to define three environmental interpretations: tidal channel, mangrove/freshwater mixed tidal zone and mangrove tidal zone (Supplementary Table 1).

### 3.1. Vegetation survey and elevation

*Rhizophora apiculata*, *R. mucronata*, *Bruguiera cylindrica*, and *Avicennia officinalis* are the predominant mangrove species along the coastal zone of Nai Nang. The vegetation changes to back mangroves, such as *Xylocarpus granatum* and *Millettia pinnata*, upstream, and embankments. These findings serve as a basis for interpreting the environmental characteristics of an area. According to FABDEM analysis, the NN-1 coring site is 2.33 m above mean sea level with predominantly features of *R. apiculata* (70%), *B. cylindrica* (20%) and *X. granatum* (10%), while the NN-2 coring site where is higher than NN-1 (5.65 m above mean sea level) and located upstream is characterized by a combination of *R. apiculata* (50%), *B. cylindrica* (20%), *M. pinnata* (20%), and *X. granatum* (10%) (Fig. 2).

### 3.2. Stratigraphy and particle size

The sedimentary sequences NN-1 and NN-2 obtained from Nai Nang mainly consist of grey silt and gradual change boundaries (Supplementary Table 1).

The lowermost sedimentary sequence NN-1 mainly consisted of grey silt, extending from 225 to 150 cm (Supplementary Table 1). Some sand fractions and undifferentiated organic materials were found in this unit. This result is consistent with the grain size analysis, suggesting 67–86% and 11–30% silt and sand fractions, respectively (Fig. 3). The sediments changed to sandy silt at 150-0 cm (Supplementary Table 1). Small fragments of woody plant roots were common in the upper layer. Grain size analysis suggested that the sand component increased to 17–45%, while the silt percentage declined to 51–80% (Fig. 3).

Sedimentary sequence NN-2 can be classified into five layers. The basal unit of NN-2 consisted of yellowish-grey sand (27–80%) and silt (12–69%) extending at 330–245 cm depth, and respectively, (Supplementary Table 1 and Fig. 3). Angular pebbles were also observed in this unit. The sand and silt components were comparable at 32–67% in the overlying layer from 245 to 150 cm depth. The silt fraction predominated at 34–92%, whereas the sand component decreased at depths of 150–130 cm. Undifferentiated organic materials, including sand and silt, were found in this layer. Woody plant roots were found in the silt and sand layers at depths of 130–110 cm. The silt fraction became dominant and was found together with woody plant roots at 130–0 cm. The boundaries between stratigraphic units were transitional. This stratigraphic description is also congruent with the grain-size distribution

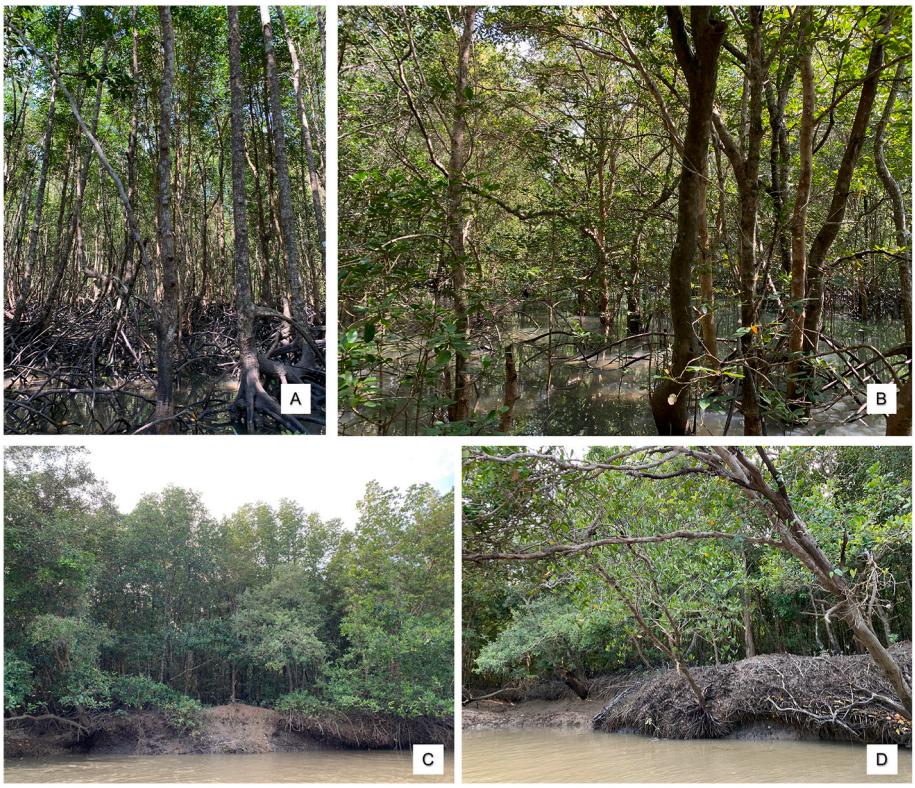


**Fig. 2.** Study site and mangrove area of the NN-1 (A–B) and NN-2 (C–D) coring sites.

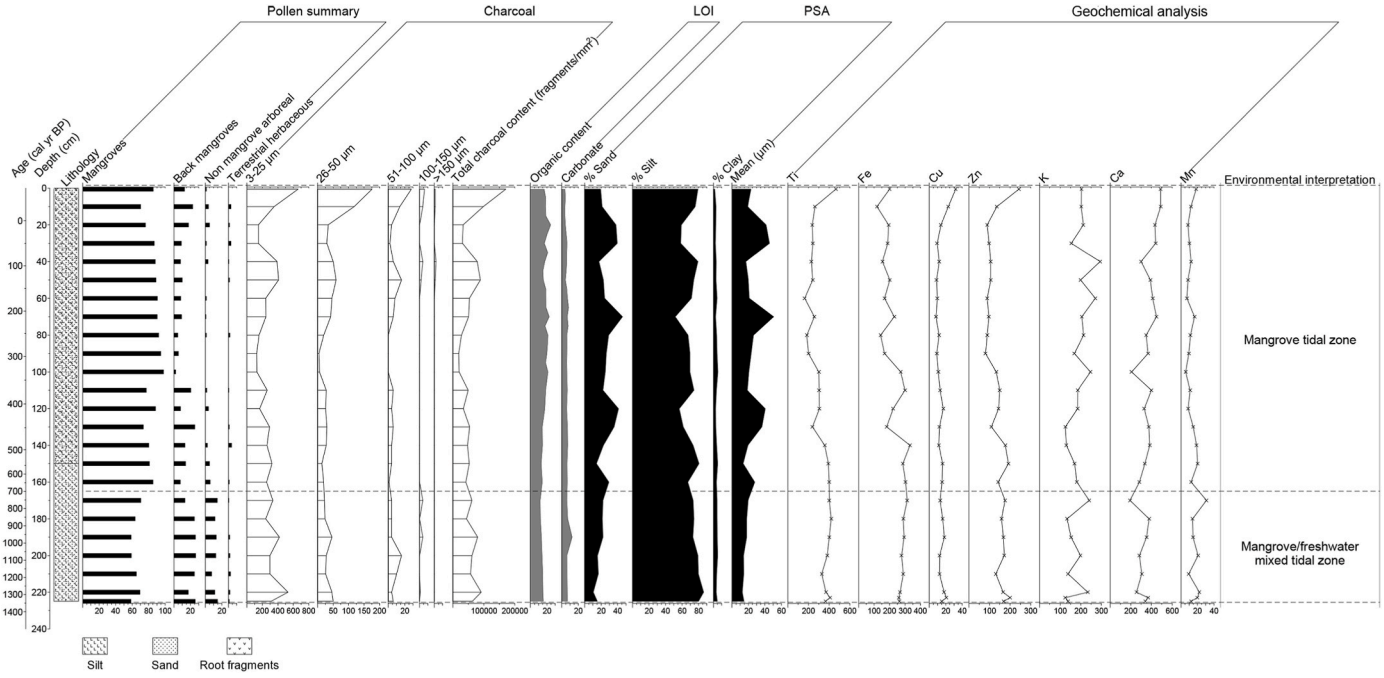


**Fig. 3.** Diagram showing pollen summary, charcoal, loss on ignition (LOI), particle size (PSA), and geochemical analyses of NN-1 core.

analysis (Fig. 4).

### 3.3. Loss on ignition and geochemical analyses

The organic carbon content in the lower part of both cores was relatively low (12–16%), while the carbonate content and geochemical analysis varied throughout both cores, as detailed in Supplementary Table 1 and Figs. 3 and 4.

### 3.4. Chronology and sedimentation rate

Seven radiocarbon dates were obtained from two cores, three from NN-1 and four from NN-2 (Table 1). Radiocarbon dating of small bark and wood fragments provides strong evidence of continuous sediment

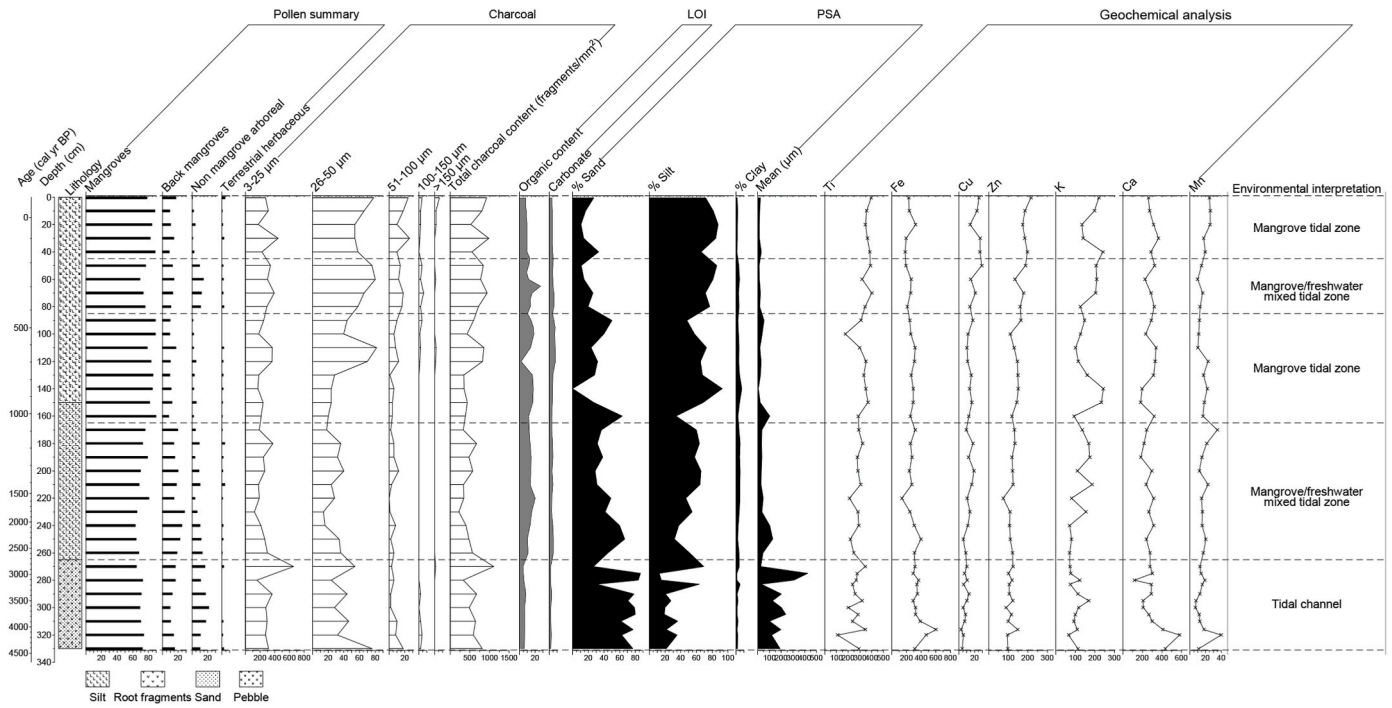


**Fig. 4.** Diagram showing pollen summary, charcoal, loss on ignition (LOI), particle size (PSA), and geochemical analyses of NN-2 core.

**Table 1**
List of radiocarbon dates from two Nai Nang cores, including calibrated age with Intcal20 curve (Reimer et al., 2020) using OxCal v4.4.4 (Bronk-Ramsey, 2021). The asterisk (*) represents the rework age and is excluded from the interpretation.

| Cores | Depth (cm) | Code | $^{14}$C yr BP | Range cal yr BP | cal yr BP | Sedimentation rates (mm year$^{-1}$) |
|---|---|---|---|---|---|---|
| NN-1 | 90 | D-AMS 047710 | 277 ± 22 | 430–157 | 294 ± 136 | 2.46 |
| NN-1 | 148 | D-AMS 047711 | 476 ± 27 | 541–496 | 518 ± 23 | 2.59 |
| NN-1 | 223 | D-AMS 046335 | 1417 ± 29 | 1355–1290 | 1318 ± 28 | 0.94 |
| NN-2 | 82 | D-AMS 049613 | 341 ± 21 | 473–315 | 394 ± 79 | 1.76 |
| NN-2 | 217 | D-AMS 047713 | 1590 ± 23 | 1528–1407 | 1467 ± 61 | 1.25 |
| *NN-2 | 270 | D-AMS 047714/ UGAMS 61572 | 3986 ± 30 | 4528–4405 | 4467 ± 62 | n/a |
| NN-2 | 325 | D-AMS 049614 | 3871 ± 27 | 4411–4158 | 4284 ± 127 | 0.38 |

accumulation and a reliable chronological sequence. However, the results obtained from the NN-2 core exhibited an older date at 270 cm, which could be attributed to sediment reworking. Despite the implementation of acid-based-acid pre-treatment to avoid the leaching of humic acids into the mangrove sequences, it is possible that the discrepancy in the dating results is attributable to the percolation of humic acids through leaching, which may have also caused the mixing of older sediments in the upper column (Hammond et al., 1991). The observed results are in line with prior studies which have reported a high occurrence of radiocarbon contamination in depositional environments characterised by high rainfall and leaching (Toscano and Macintyre, 2003; Newnham et al., 2007). Consequently, six radiocarbon dates (excluding the date obtained from 270 cm of NN-1) were used to establish a chronology for the palaeoecological interpretation. The detailed age-depth relationships of cores NN-1 and NN-2 are shown in Fig. 5. The sedimentation rates of both cores were characterised by higher sediment accumulation towards the core top.

### 3.5. Pollen analysis

Pollen analysis of cores NN-1 and NN-2 was performed, and pollen taxa were grouped into ecological categories, including mangroves, back mangroves, terrestrial herbaceous, non-mangrove arboreal, and unknown taxa. Pteridophyte and algae spores were present in the pollen diagram, but were excluded from the pollen sum.

#### 3.5.1. Pollen diagram description of NN-1 core

Pollen zones were divided into three main zones (NN-1a, NN-1b, and NN-1c) and six subzones as follows.

*3.5.1.1. Zone NN-1a-1 (225–165 cm: 1340–700 cal yr BP).* Pollen zone NN-1a was dominated by mangroves (58–70%, Fig. 6), followed by back mangroves (7–26%), non-mangrove arboreal taxa (5–14%), and terrestrial herbaceous taxa (0–2.5%).

*Rhizophora* was the prominent mangrove pollen taxa, followed by *Brugueira/Ceriops*. However, they had the lowest percentage compared to those in the NN-1b and NN-1c zones. The back mangrove taxa dominated by *Millettia*, *Acrostichum*, *Oncosperma*, and *Stenochlaena*, and non-mangrove arboreal taxa characterised by *Elaeocarpus* were relatively higher than the other two zones, with a short increase between 220 and 210 cm.

*3.5.1.2. Zone NN-1a-2 (165–145 cm: 700–500 cal yr BP).* The mangrove taxa gradually increased, reaching 85% in this zone. However, back mangroves (13%), dominated by *Millettia* (5%), and non-mangrove arboreal taxa decreased toward the top of zone NN-1a-2.

*3.5.1.3. Zone NN-1b (145–105 cm: 500–350 cal yr BP).* The mangrove taxa dominated by *Rhizophora* and back mangrove taxa were 73–88% and 7–22%, respectively, that were comparable to the top of the NN-1a

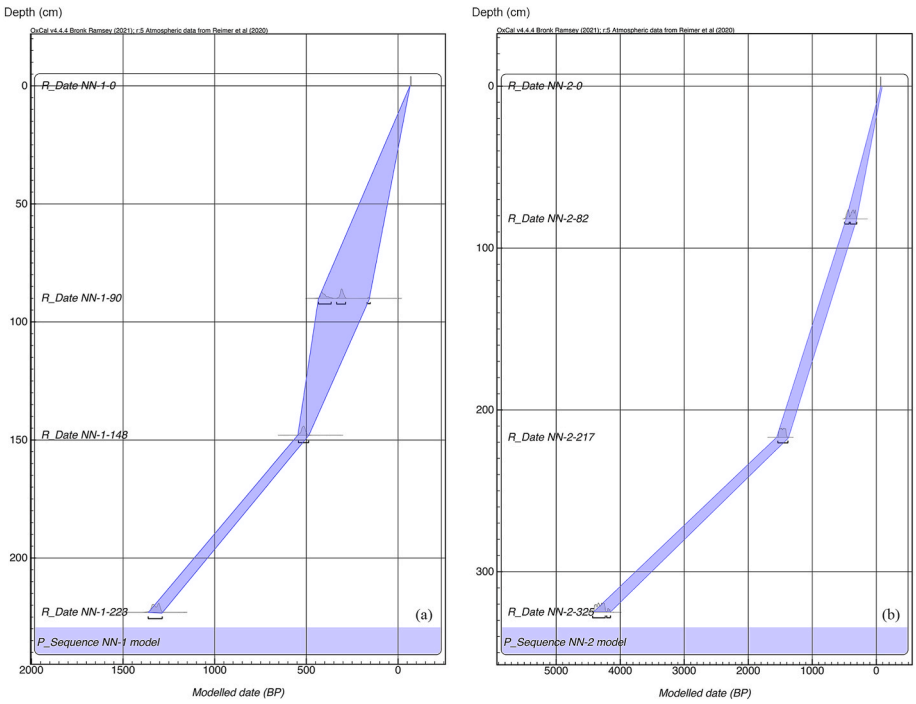


**Fig. 5.** Age-depth model using OxCal v4.4.4 (a) NN-1 core and (b) NN-1 core.

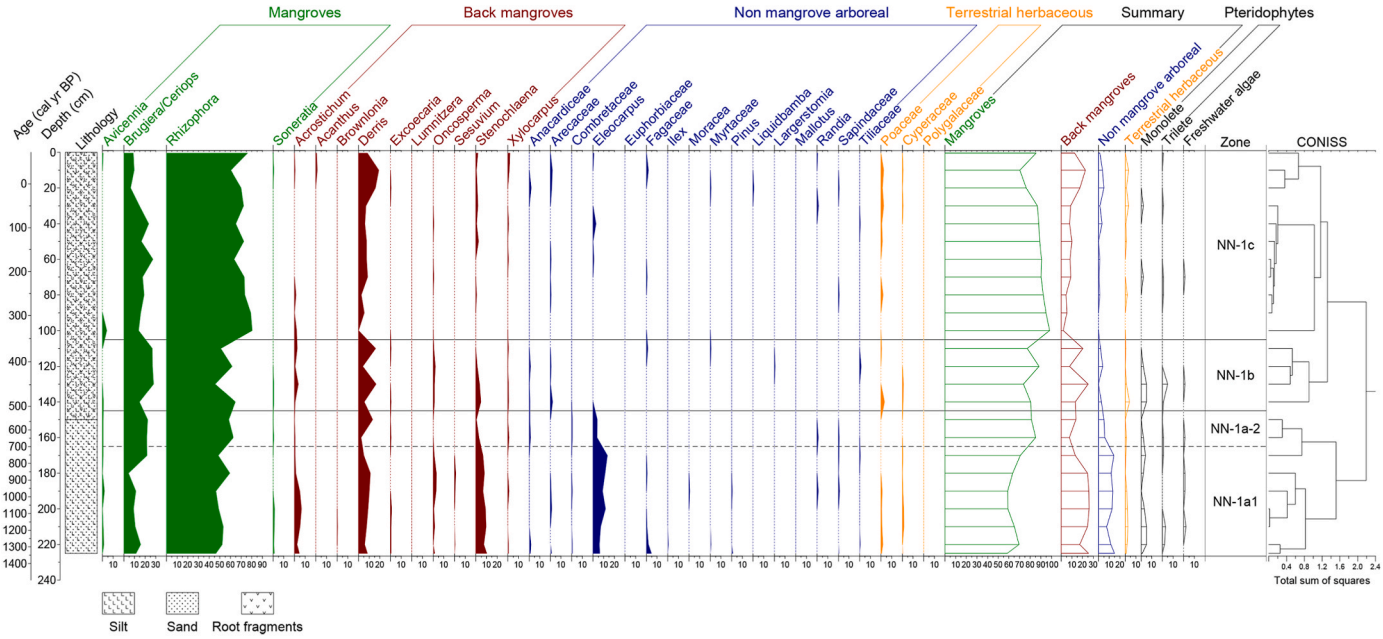


**Fig. 6.** Pollen diagram presented as percentages of the total pollen sum of the NN-1 core.

zone. However, the abundance of non-mangrove arboreal taxa decreased by less than 4%. *Elaeocarpus*, the dominant non-mangrove arboreal pollen taxon in zones NN-1a-1 and NN-1a-2, was undetectable.

*3.5.1.4. Zone NN-1c (105–0 cm: 350 cal yr BP to present).* Zone NN-1c was also an abundance of 70–98% mangrove pollen taxa, especially *Rhizophora*, followed by *Brugueira/Ceriops* and *Avicennia* at the bottom of this zone. Back mangroves, particularly *Millettia*, decreased by 2–22%. The non-mangrove arboreal and terrestrial herbaceous taxa were insignificant in this zone. At 20–10 cm, the back mangrove, non-mangrove arboreal, and terrestrial herbaceous pollen taxa increased, whereas mangrove pollen taxa diminished. An increase in mangrove pollen taxa was observed at the top of this zone.

### *3.5.2. Pollen diagram description of NN-2 core*

Pollen zones were divided into three main zones (NN-2a, NN-2b, and NN-2c) and six subzones as follows.

*3.5.2.1. Zone NN-2a-1 (330–265 cm: 4410–2720 cal yr BP).* Pollen zone NN-2a-1 mainly consisted of 72% of mangrove pollen taxa before declining to 64% at the top of this zone (Fig. 7). *Rhizophora* was the most abundant mangrove pollen taxon of 54–67%, followed by the higher-

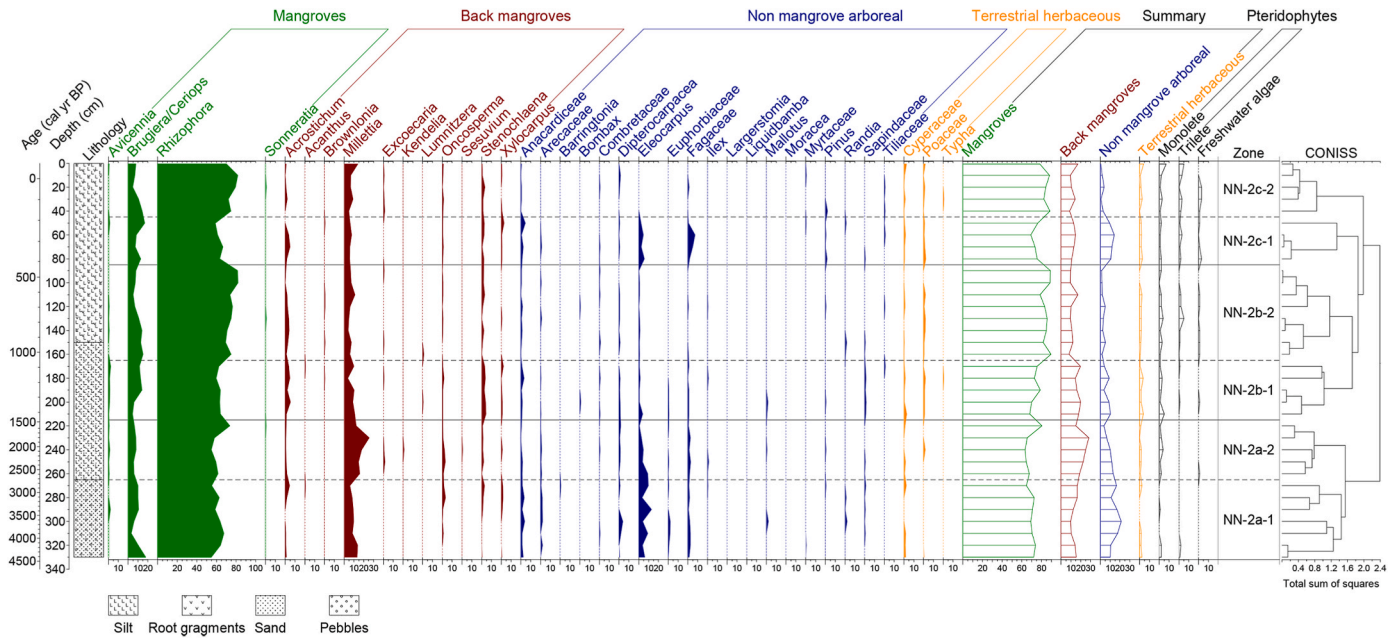


**Fig. 7.** Pollen diagram presented as percentages of the total pollen sum of the NN-2 core.

intertidal species of *Brugueira/Ceriops* (3–17%). Non-mangrove arboreal pollen taxa were 11–21% and the highest percentage compared to the other zones in core NN-2. *Elaeocarpus* accounted for 4–12% and was the most dominant non-mangrove arboreal, followed by Anacardiaceae, Fagaceae, and Arecaceae. The back mangrove pollen taxa were slightly changed by 9–16%, especially *Millettia*, followed by *Acrostichum*, *Oncosperma*, and *Stenochlaena*. The terrestrial herbaceous pollen taxon, mainly composed of Cyperaceae, was relatively small.

*3.5.2.2. Zone NN-2a-2 (265–215 cm: 2720–1450 cal yr BP).* In this zone, mangrove pollen taxa were relatively constant at 63–67%. They were dominant in *Rhizophora*, followed by *Brugueira/Ceriops* and *Avicennia*. Mangrove pollen increased to 80% at the top of this zone. The back mangrove pollen taxa, particularly *Millettia*, were 17–28% higher than those in zone NN-2a-1. The non-mangrove arboreal taxon, mainly *Elaeocarpus*, gradually declined to 3–16%. Terrestrial herbaceous pollen was very low and dominant in Cyperaceae.

*3.5.2.3. Zone NN-2b-1 (215–165 cm: 1450–1050 cal yr BP).* A slight increase in mangrove pollen taxa was observed, with an insignificant change of 69–78%. *Rhizophora* and *Brugueira/Ceriops*, and *Avicennia* increased from the bottom to the top of this zone. Although *Acrotichum* and *Stenochlaena* spores increased, the decrease in *Millettia* resulted in mangrove pollen taxa of 15–20%, which was lower than that in the underlying pollen zones. The non-mangrove arboreal taxa Anacardiaceae, Fagaceae, Dipterocarpaceae, and Elaeocarpus were present at 3–11%. The terrestrial herbaceous taxa, mainly Poaceae and Cyperaceae, were slightly higher than those in the previous zones.

*3.5.2.4. Zone NN-2b-2 (165–85 cm: 1450–420 cal yr BP).* Mangrove pollen taxa, especially *Rhizophora* and *Brugueira/Ceriops*, were 79–90% and increased toward the top of this zone. The back mangrove (i.e., *Millettia*, *Acrotichum*, and *Stenochlaena*) and non-mangrove arboreal (i.e., Anacardiaceae, Dipterocarpaceae, and *Elaeocarpus*) pollen taxa were slight changes of 8–12% and 1–5%, respectively. Terrestrial herbaceous pollen taxa, consisting of Poaceae and Cyperaceae, decreased by 2–5% and disappeared toward the top of this zone.

*3.5.2.5. Zone NN-2c-1 (85–45 cm: 420–180 cal yr BP).* Mangrove pollen taxa were comparable to those in zone NN-2b-1. *Rhizophora* and *Brugueira/Ceriops* pollen increased at the top of this zone. The back mangrove pollen taxa *Millettia*, *Acrotichum*, and *Stenochlaena* were 11–15%. However, the non-mangrove pollen arboreal increased to 11–14%, particularly 2–5% of *Elaeocarpus* and 1–7% of Fagaceae. Terrestrial herbaceous pollen taxa, that is Poaceae and Cyperaceae, increased by 1–3%.

*3.5.2.6. Zone NN-2c-1 (45–0 cm: 180 cal yr BP to present).* Zone NN-2c-1 contained the higher abundance of mangrove pollen taxa, 78–88%. Mangrove pollen decreased and was occupied by back mangrove pollen, that is, *Millettia*, *Acrotichum*, and *Stenochlaena*. *Elaeocarpus*, non-mangrove arboreal pollen, disappeared. Non-mangrove arboreal pollen was meager in this zone.

### 3.6. Charcoal analysis

The charcoal fragments from the NN-1 and NN-2 cores were counted in each size class, calculated in terms of total charcoal content, and presented as a charcoal diagram shown in Figs. 3 and 4. The charcoal zones were divided based on the environmental interpretation zones. The presence of larger particles was significantly higher at the top of both cores (Supplementary Table 1).

### 3.7. Principle component analysis (PCA)

The PCA included sediment components, pollen percentages, and significant geochemical components (Ti, Fe, K, and Ca). The first three components of the PCA scores explained 63.8% of the cumulative variance. The eigenvalues of axes 1, 2, and 3 are 4.6, 3.3, and 1.7, respectively (Fig. 8). Therefore, the PCA of axes 1, 2, and 3 was used to identify the drivers of environmental changes. According to the factor loading, these data can be classified into three clusters: A, B, and C along PCA axes 1, 2, and 3, respectively. Based on the PCA, cluster A was along PCA axis 1, with 30.74% of the total variance. It comprises percentages of Ti, Ca, K, Fe, and silt and sand fractions. The reverse relationship between Fe and other major elements, particularly Ti, demonstrates the possibility of exposure and oxidation reflected in the water level shift. This possibility was supported by the opposition between sand and silt. PCA axis 2 accounted for 21.88% of the total variance and was composed of members of cluster B, that is, sediment components and

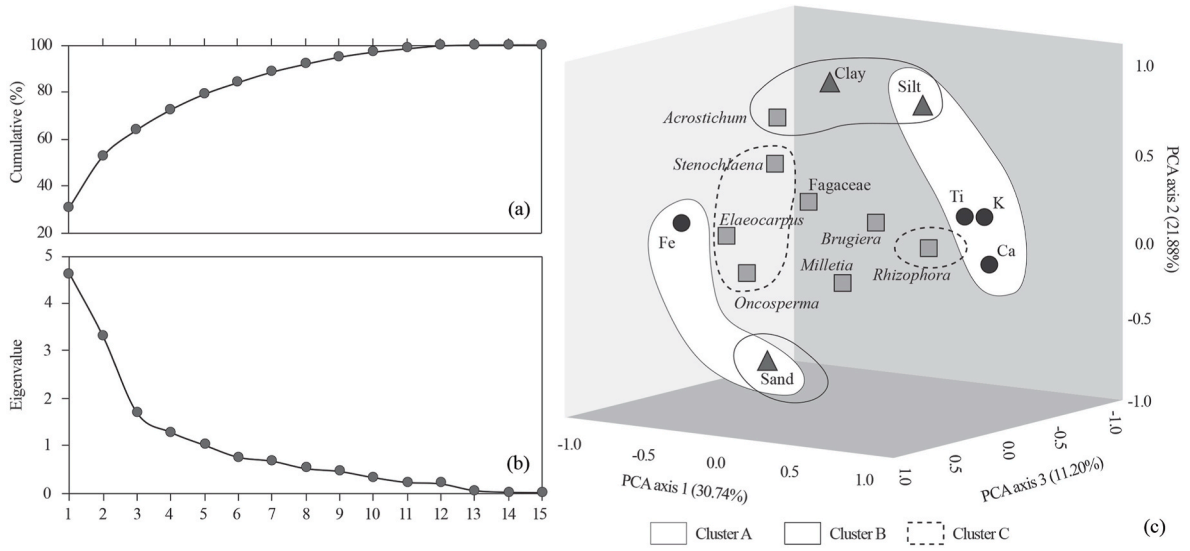


**Fig. 8.** PCA showing (a) the first three components of The PCA scores explained 63.8% of the cumulative variance; (b) the eigenvalues of axes 1, 2, and 3 were 4.6, 3.3, and 1.7, respectively; (c) the PCA of axes 1, 2, and 3 were considered to identify the drivers of environmental changes classified into three clusters: clusters A, B, and C, respectively.

*Acrostichum*. The consistent presence of silt and clay fractions opposed the sand content, indicating a low runoff intensity. Cluster C accounted for 17% of the total variance and consisted of non-mangrove pollen taxa (*Oncosperma*, *Elaeocarpus*, and *Stenochlaena*) and a mangrove pollen taxon (*Rhizophora*). This cluster of non-mangrove taxa suggests expansion or shrinkage of mangrove forests.

## 4. Discussion

Multi-proxy analysis results, including data from pollen, charcoal, stratigraphy, particle size, and geochemical analyses of two cores from Nai Nang, Krabi, were used to reconstruct vegetation dynamics and coastal environments over the past 4400 cal yr BP. Although it is not feasible to synthesise data from the two cores into a composite dataset, owing to a significant distance of approximately 750 m between bore holes, the results demonstrate consistency across the study site. The findings indicate that vegetation dynamics in this region were shaped by a combination of RSL and climate change, human interaction (allogenic processes), as evidenced by the pollen and charcoal results, as well as local sedimentary dynamics (autogenic processes). Pollen analysis consistently revealed mangrove dominance in both cores. While variations in rainfall patterns influenced by monsoon dynamics play a pivotal role in determining freshwater runoff, sediment transport, and nutrient influx into the mangrove ecosystem impacting salinity and overall composition, it appears that the primary driver of mangrove expansion in Nai Nang is linked to sea-level changes. Nevertheless, it is important to note that a study suggests a potential connection between seasonal sea-level variations and monsoon patterns in the Andaman Sea (Brown et al., 2011). Consequently, the synthesis of pollen and charcoal data, along with the correlation between sediment components and geochemical analysis, facilitates an interpretation that can be delineated into three distinct phases:(i) a phase when tidal channels dominated the area (~4400–~2700 cal yr BP), (ii) a phase when mangrove/freshwater influences were mixed across the tidal area (~2700–~1050 cal yr BP), and (iii) a phase where mangroves dominated the tidal area (~1050 to present) (Fig. 9).

### 4.1. Tidal channels dominating (~4400–~2700 cal yr BP)

This phase was recorded in core NN-2, where the presence of angular pebbles as bedding and the prevalence of sandy sediments suggests a relatively high-energy depositional environment, indicative of sediment accumulation from the tidal channel. This is supported by a study of the geomorphology of the area, which indicates that Nai Nang is characterised by recent mangrove deposits overlying Pleistocene-Holocene colluvial and alluvial sediments (Somsak and Jantakham, 2013). Pollen analysis in zone NN-2a-1 showed dominant mangroves characterized by *Rhizophora*, indicating mangrove development since ~4400 cal yr BP under tidal influence. However, freshwater input also affected the area supporting back mangrove taxa and freshwater forest species such as *Elaeocarpus*. The contemporary distribution of *Elaeocarpus*, particularly *E. macrocerus* and *E. grandiflorus*, is found in the Malay-Thai Peninsula in freshwater swamps or along streams (Phengklai, 1981). High concentrations of Fe and fluctuating levels of Ti, which represent terrigenous sediments produced by fluvial and eolian processes (Bahr et al., 2005; Nace et al., 2014; Gebregiorgis et al., 2020), could reflect fluvial influences in the area. Therefore, the sedimentary features and pollen results suggest that core NN-2 was a shallow tidal channel that allowed mangrove/freshwater mixed vegetation to establish from ~4400 to ~2700 cal yr BP (Fig. 9). At the bottom, a thick deposit of sand filled the tidal channel, followed by a layer of muddy sediment from the intertidal zone. The sediment in the intertidal zone had distinct patterns of wavy and lenticular bedding at the base and top of zone NN-2a-1, respectively, and was covered by mangrove/freshwater mixed vegetation situated adjacent to estuarine or tidal channels. The results obtained during the period of 4400–2700 cal yr BP suggest a slight sea-level rise from 4400–4200, followed by a low sea level onwards, as reflected by the high and then low levels of *Rhizophora* and Ca contents as Ca intensities were produced by marine plankton (Bahr et al., 2005; Nace et al., 2014; Gebregiorgis et al., 2020). Our findings align with previous studies of sea-level changes in both the Andaman Sea (Tjia, 1996; Fujimoto et al., 1999; Scheffers et al., 2012) and the Gulf of Thailand coast (Pramojanee et al., 1986; Horton et al., 2005). These studies collectively demonstrate that sea levels reached a highstand at approximately 4000 cal yr BP, before gradually declining. This pattern is consistent with broader regional evidence from the west coast of Malaysia and Singapore, which indicates that a highstand occurred during the period of approximately 5100–4000 cal yr BP (Mann et al., 2019; Chua et al., 2021). Based on the elevation data from the Digital Elevation Model (DEM) of NN-1, the NN-1 area is approximately 2 m lower than the NN-2 area, suggesting that the NN-1 area likely constituted a shallow sea during this period (Fig. 9). These findings highlight the intricate interplay between the

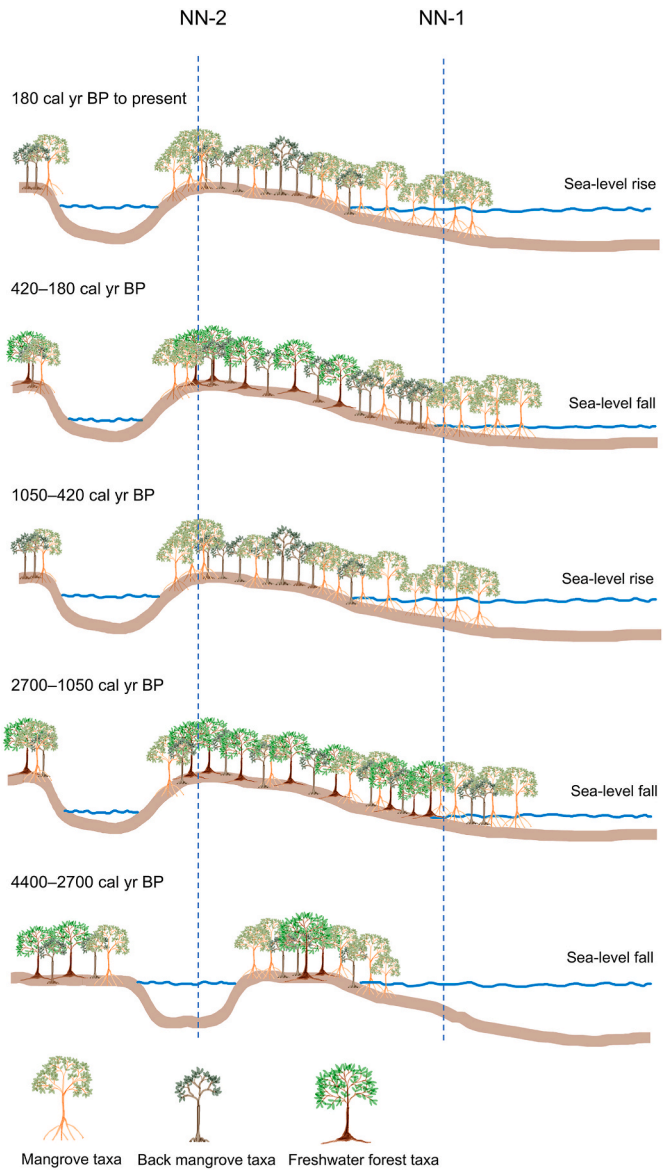


**Fig. 9.** Model of Nai Nang coastal dynamics influencing mangrove establishment.

environmental factors and vegetation dynamics in mangrove ecosystems. The differences in dominance timing between cores NN-1 and NN-2 underscore the importance of considering the local topography and elevation when interpreting paleoenvironmental records. Furthermore, this assumption is supported by the stratigraphy of the NN-1 core, which indicates the presence of impenetrable compact grey mud, indicative of marine deposition. The low sedimentation rate of 0.38 mm year-1, coupled with a low organic content, may also be attributed to a low sea level during 4200–2700 cal yr BP.

There was a notable presence of high charcoal content between 4400 and 2700 cal yr BP, primarily consisting of charcoal particles ranging from 25 to 100 μm, with occasional occurrences of particles in the 100–150 μm size range. The significant abundance of charcoal suggests increased fires that are likely linked to a prevailing drought during the mid-Holocene, as observed from lake records in northeastern Thailand, which indicate a dry period extending from ~6500 to 2700 cal yr BP (Chawchai et al., 2015), and from records from Cambodia (Maxwell, 2001, 2004). These dry conditions can be attributed to the weakening of the Asian summer monsoon during the mid-Holocene, which led to a reduction in precipitation (Chawchai et al., 2015; Wohlfarth et al., 2016). This result is consistent with marine geochemical records from the Andaman and Arabian Seas (Sarkar et al., 2000), which also indicate decreased precipitation from 6000 to 3500 cal yr BP. Additionally, elevated charcoal content was observed in the NN-2 core, potentially due to climatic extremes associated with a climate change event that affected the tropics between 5000 and 4000 cal yr BP, characterised by arid conditions across equatorial Asia and Africa (Marchant and Hoogh-iemstra, 2004; Griffiths et al., 2020).

### 4.2. *Mangrove/freshwater mixed tidal area (~2700–~1050 cal yr BP)*

After ~2700 cal yr BP, sediments changed from sand deposited in subtidal channels (zone NN-2a-2) to intertidal silt (zone NN-2b-1). Based on the upward fining of the sediments, we suggest that the channel was filled through lateral migration associated with tidal activity and freshwater input related to low-energy environments. The establishment of subsequent intertidal flats in Nai Nang provides a stable setting that supports vegetation growth and expansion under the influence of brackish water (Ribeiro et al., 2018).

The prevalence of mangroves, characterised by *Rhizophora*, in core NN-2 exhibited a relative decrease, while the back mangrove taxa increased from 2700 to 1050 cal yr BP. These shifts in plant composition were indicative of reduced seawater inundation, thereby suggesting that the corresponding sea level was lower during this period. This sea-level regression was also supported by the lower Ca and higher Ti values, reflecting less marine influence in Nai Nang. Pollen analysis suggested that mangroves, back mangroves, and freshwater forests thrived adjacent to Nai Nang during this period. This result supports the environmental transformation from the tidal channel to the intertidal flat until 1050 cal yr BP (Fig. 9). The replacement of the mangrove/freshwater mixed tidal flat reconstructed in core NN-2 occurred slightly later in zone NN-1a-1 obtained from core NN-1, which was 1300 cal yr BP. However, the significant increase in mangrove pollen taxa associated with the decline in back mangrove and non-mangrove arboreal taxa in zone NN-2a-2 indicates an excursion of sea-level rise from ~1570 to ~1400 cal yr BP. The sea level fall in Nai Nang at approximately 2700–1050 cal yr BP is consistent with a late Holocene regression that has been reconstructed along the Andaman coast (Fujimoto et al., 1999; Scheffers et al., 2012) and the western Gulf of Thailand (Pramojanee et al., 1986). Additionally, investigations conducted along the east coast of Malaysia have reported lower sea levels from ~2300 to 800 cal yr BP (Tam et al., 2018).

Furthermore, starting from approximately 2700 cal yr BP, there was a noticeable decline in charcoal content, accompanied by the disappearance of large charcoal fragments. These observations suggest decreased fire activity, which is probably related to a shift towards wetter conditions, coinciding with a gradual increase in summer monsoon activity across the Southeast Asian mainland, including northeastern Thailand. This shift in charcoal content aligns with the findings reported by Chawchai et al. (2015), Wohlfarth et al. (2016), and Griffiths et al. (2020) could potentially influence the northward shift of the Intertropical Convergence Zone (ITCZ) in regional climate dynamics (Chawchai et al., 2015). These results are consistent with findings from marine records from the Andaman Sea and Arabian Sea, which suggest an intensification in precipitation during the period 3500–2000 cal yr BP (Sarkar et al., 2000). The increased humidity persisted until approximately 1350–1200 cal yr BP, when both the NN-1 and NN-2 cores exhibited an increase in charcoal content, indicating increased fire regimes, probably due to a brief period of drier conditions. This likely corresponds to the recorded moisture availability during 2100–1700 cal yr BP, followed by a drier phase during 1700–1100 cal yr BP in northeastern Thailand (Wohlfarth et al., 2016). However, it is important to note that our record of the dry period occurred later and was of a shorter duration (approximately 1350–1200 cal yr BP) before transitioning back to wetter conditions (Wohlfarth et al., 2016).

### 4.3. Mangrove tidal area (~1050 to present)

The sediments in this phase were dominated by silt in cores NN-1 and NN-2, similar to the previous interval, and likely to have been deposited under low-energy intertidal conditions. Mangrove pollen taxa, especially *Rhizophora*, followed by *Bruguiera* increased, whereas freshwater pollen taxa were greatly reduced. Pollen analysis indicated a succession of mangrove forest and replacement of mixed vegetation at 1050 cal yr BP in core NN-2 and ~800 cal yr BP in core NN-1, possibly indicating sea-level rise (Fig. 9). This observation was further substantiated by the elevated sedimentation rate, which is likely a consequence of expanded mangrove vegetation, leading to increased sediment accumulation as a result of rising sea levels. These results also correspond with records along the Andaman coast after approximately 1000 cal yr BP (Fujimoto et al., 1999; Scheffers et al., 2012) and in the eastern Gulf of Thailand at 1300–500 cal yr BP (Englong et al., 2019), indicating sea-level rise. However, our findings cannot be directly compared with those of other areas of the Malay-Thai Peninsula and Singapore because of the lack of recorded sea-level index points beyond 800 cal yr BP (Tam et al., 2018; Chua et al., 2021).

It should be noted that in core NN-2, which is located higher than core NN-1, the mangrove pollen taxa decreased, whereas *Elaeocarpus*, a freshwater species, increased at ~420-180 cal yr BP. This result demonstrates the reoccurrence of mangrove/freshwater mixed tidal vegetation, reflecting the intervention of sea-level fall at ~420–180 cal yr BP. Although the decrease in sea level during this period was not recorded elsewhere along the Andaman coast, it is consistent with records from the Gulf of Thailand at approximately 500–200 cal yr BP (Horton et al., 2005; Englong et al., 2019) and 700–200 cal yr BP (Punwong et al., 2018, 2023). The dominance of mangrove pollen taxa towards the core tops in NN-1 and NN-2 indicated continued sea-level rise. The latest observations of sea-level rise in this area over the last 180 cal yr BP align with a study conducted on the Andaman Sea coast between 1972 and 2011, which revealed increasing sea-level rise rates ranging from 6.7 mm $year^{-1}$ to 3.9 mm $year^{-1}$ in Krabi (1981–2011 CE) (Putcharapitchakon and Ritphring, 2012).

The charcoal concentrations in cores NN-1 and NN-2 decreased from approximately 1050 to 700 cal yr BP, suggesting decreased fires, possibly due to wet conditions. This result is consistent with evidence from northeastern Thailand between ~1150 and 1000 cal yr BP (Chawchai et al., 2015; Wohlfarth et al., 2016; Yamoah et al., 2017). Furthermore, tree-ring studies in Southeast Asia also indicated the strengthening of summer monsoons at approximately 900–850 cal yr BP (Buckley et al., 2010, 2014). Moreover, the pollen record from the eastern Gulf of Thailand suggests the presence of wet conditions associated with a more vigorous summer monsoon at approximately 1500–700 cal yr BP (Englong et al., 2019). The increased charcoal content, particularly in core NN-2, indicates increased fires, probably related to lower moisture availability from ~700 to 500 cal yr BP. The drier conditions were consistent with the records in the eastern Gulf of Thailand (Englong et al., 2019) and northeast Thailand (Chawchai et al., 2015), and contemporary with the Medieval Climate Anomaly in Southeast Asia (Lieberman and Buckley, 2012), indicating weakening of the summer monsoon (Wohlfarth et al., 2016; Yamoah et al., 2017). Additionally, an increase in large charcoal fragments (>100 μm) was observed during this period, suggesting potential local fires caused by human activities in the surrounding area. Following 500 cal yr BP, the charcoal concentration fluctuated, possibly associated with unstable climatic conditions across mainland Southeast Asia (Buckley et al., 2010, 2014; Cook et al., 2010; Lieberman and Buckley, 2012; Punwong et al., 2018, 2021), although dry conditions prevailed during most of this period in northeast of Thailand (Wohlfarth et al., 2016; Yamoah et al., 2017). In addition, the topmost part of both cores showed high charcoal content, particularly due to their larger size, which is likely indicative of human activities in the surrounding area, although there is no evidence of domesticated pollen records in the cores.

### 4.4. Mangrove vulnerability to future sea-level rise

Mangrove sediment accumulation provides valuable insights into the adaptive capacity of mangroves in response to sea-level rise (Ellison, 2015). The pollen records obtained from the Krabi region demonstrate the adaptability of mangroves to sea-level changes over the past 4400 years. The average sedimentation rates of 0.38–2.59 mm $year^{-1}$ observed in the area suggest that mangroves in Krabi may have not been able to keep pace with the current rates of sea-level rise in the Andaman Sea (Putcharapitchakon and Ritphring, 2012). However, it is crucial to consider the projected increase in global sea-level rise, which estimates a potential range of 3.0–13.2 mm $year^{-1}$ (Horton et al., 2020). Based on these projections, it is anticipated that mangroves in Krabi will need to undergo significant landward migration to cope with increasing sea-level rise. The ability of mangroves to migrate landward is essential for the long-term survival and maintenance of ecosystem functions and the provision of vital services from carbon storage to fisheries. Landward migration allows mangroves to keep pace with rising sea levels and to establish new habitats in suitable areas. Understanding the migratory responses of mangroves to sea-level rise is crucial for effective coastal management and conservation efforts. Further research should focus on assessing the potential for landward migration of mangroves in Krabi and identifying suitable areas for their future establishment. This information can inform conservation strategies, land-use planning, and the implementation of adaptive management practices to ensure the persistence and resilience of mangrove ecosystems in the face of ongoing and projected sea-level rise.

## 5. Conclusion

The multi-proxy analysis indicates that Nai Nang along the Krabi coast underwent significant changes in vegetation and sedimentary dynamics during the late Holocene. The site evolved from being dominated by tidal channels to a mangrove/freshwater mixed influence and was eventually dominated by mangrove ecosystems. These changes were driven by a combination of allogenic processes, such as relative sea-level and climate changes, and autogenic processes related to local sedimentary dynamics. During the tidal channel phase (~4400–~2700 cal yr BP), the site was characterised by high-energy depositional environments. Mangrove development began around 4400 cal yr BP and was influenced by tidal regime and freshwater input. Sea-level fluctuations during this period showed a slight increase, followed by low sea level under dry environmental conditions. The mangrove/freshwater mixed tidal area phase (~2700–1050 cal yr BP) was characterised by the filling of the tidal channel with finer sediments and the establishment of intertidal flats through lateral migration. The presence of mangroves, back mangroves, and freshwater forest taxa indicates a transition to a mixed vegetation type and a relatively low sea level during this period. In the mangrove tidal area phase (~1050 to present), mangroves have replaced more mixed vegetation. The sea level rose during this period, resulting in an increased dominance of mangroves in the study area. Human activities potentially contributed to the high charcoal content observed in recent layers. These findings highlight the complex interplay among environmental factors, sea-level fluctuations, human interaction and vegetation dynamics in driving mangrove ecosystem composition and distribution. The records of mangrove responses to sea-level changes over the past 4400 years provide valuable insights into their adaptive capacity. However, the current rates of sea-level rise may exceed the ability of mangroves in the study area to keep pace, necessitating landward migration. This information is essential for coastal conservation and management. Further research should focus on assessing the potential for mangrove migration and identifying suitable areas for their future establishment to ensure their long-term survival and resilience in the face of ongoing sea-level rise.

## Declaration of competing interest

The authors declare that they have no known competing financial interests or personal relationships that could have appeared to influence the work reported in this paper.

## Data availability

No data was used for the research described in the article.

## Acknowledgments

We would like to express our gratitude to the Faculty of Environment and Resource Studies of Mahidol University and the Department of Environment and Geography of the University of York, who provided all the required equipment and materials to achieve this work. We would like to express our appreciation to the Department of Marine and Coastal Resources, Ministry of Natural Resources and Environment, for facilitating access to the mangrove area. We also extend our heartiest thank N. Photong, S. Anglong, and K. Anglong provided fieldwork assistance. This research project is supported by Mahidol University.

## Appendix A. Supplementary data

Supplementary data to this article can be found online at https://doi.org/10.1016/j.qsa.2023.100133.

## References

Admiralty Tide Tables, 2014. NP203 Admiralty Tide Tables (ATT), Vol 3 Indian Ocean (Including Tidal Stream Tables). United Kingdom Hydrographic Office.
Bahr, A., Lamy, F., Arz, H., Kuhlmann, H., Wefer, G., 2005. Late glacial to Holocene climate and sedimentation history in the NW Black Sea. Mar. Geol. 214 (4), 309–322. https://doi.org/10.1016/j.margeo.2004.11.013.
Bronk Ramsey, C., 2021. OxCal v4.4.4.Available at https://c14. arch.ox.ac.uk/oxcal.html..
Brown, B.E., Dunne, R.P., Phongsuwan, N., Somerfield, P.J., 2011. Increased sea level promotes coral cover on shallow reef flats in the Andaman Sea, eastern Indian Ocean. Coral Reefs 30, 867–878. https://doi.org/10.1007/s00338-011-0804-9.
Buckley, B.M., Anchukaitis, K.J., Penny, D., Fletcher, R., Cook, E.R., Sano, M., Nam, L.C., Wichienkeeo, A., Minh, T.T., Hong, T.M., 2010. Climate as a contributing factor in the demise of Angkor, Cambodia. Proc. Natl. Acad. Sci. USA 107 (15), 6748–6752. https://doi.org/10.1073/pnas.0910827107.
Buckley, B.M., Fletcher, R., Wang, S.Y.S., Zottoli, B., Pottier, C., 2014. Monsoon extremes and society over the past millennium on mainland Southeast Asia. Quat. Sci. Rev. 95, 1–19. https://doi.org/10.1016/j.quascirev.2014.04.022.
Chawchai, S., Chabangborn, A., Fritz, S., Väliranta, M., Mörth, C.M., Blaauw, M., Reimer, P.J., Krusic, P.J., Löwemark, L., Wohlfarth, B., 2015. Hydroclimatic shifts in north-east Thailand during the last two millennia–The record of Lake Pa Kho. Quat. Sci. Rev. 111, 62–71. https://doi.org/10.1016/j.quascirev.2015.01.007.
Chua, S., Switzer, A.D., Li, T., Chen, H., Christie, M., Shaw, T.A., Khan, N.S., Bird, M.I., Horton, B.P., 2021. A new Holocene sea-level record for Singapore. Holocene 31 (9), 1376–1390. https://doi.org/10.1177/09596836211019096.
Chumchim, N., 2010. Palynology of Mangrove Flora in Thailand. Masters thesis. Chulalongkorn University, Bangkok, Thailand.
Clark, J.S., Royall, P.D., 1995. Particle-size evidence for source areas of charcoal accumulation in late Holocene sediments of eastern North American lakes. Quat. Res. 43 (1), 80–89. https://doi.org/10.1006/qres.1995.1008.
Climate Center, 2023. Climate by Province. Thai Meteorological Department. http://climate.tmd.go.th/data/province/. (Accessed 5 February 2023).
Cook, E.R., Anchukaitis, K.J., Buckley, B.M., D'Arrigo, R.D., Jacoby, G.C., Wright, W.E., 2010. Asian monsoon failure and megadrought during the last millennium. Science 328 (5977), 486–489. https://doi.org/10.1126/science.1185188.
Department of Marine and Coastal Resources, 2018. Marine and coastal resource data of Krabi Province. In: Department of Marine and Coastal Resources. Ministry of Natural Resources and Environment in Thai.
Ellison, J.C., 2015. Vulnerability assessment of mangroves to climate change and sea–level rise impacts Wetl. Ecol. Manag. 23, 115–137. https://doi.org/10.1007/s11273-014-9397-8.
Englong, A., Punwong, P., Selby, K., Marchant, R., Traiperm, P., Pumijumnong, N., 2019. Mangrove dynamics and environmental changes on Koh Chang, Thailand during the last millennium. Quat. Int. 500, 128–138. https://doi.org/10.1016/j.quaint.2019.05.011.
Englong, A., Punwong, P., Marchant, R., Seelanan, T., Wynne-Jones, S., Chirawatkul, P., 2023. High-Resolution multiproxy record of environmental changes and anthropogenic activities at unguja ukuu, zanzibar, Tanzania during the last 5000 years. Quaternaria 6 (1), 21. https://doi.org/10.3390/quat6010021.
Faegri, K., Iversen, J., 1989. Textbook of Pollen Analysis. Wiley&Sons, Chichester.
Fujimoto, K., Miyagi, T., Murofushi, T., Mochida, Y., Umitsu, M., Adachi, H., Pramojanee, P., 1999. Mangrove habitat dynamics and Holocene sea-level changes in the southwestern coast of Thailand. Trop 8, 239–255.
Gebregiorgis, D., Giosan, L., Hathorne, E.C., Anand, P., Nilsson-Kerr, K., Plass, A., Lückge, A., Clemens, S.C., Frank, M., 2020. What can we learn from X-ray fluorescence core scanning data? A paleomonsoon case study. G-cubed 21 (2). https://doi.org/10.1029/2019GC008414 e2019GC008414.
Gilman, E.L., Ellison, J., Duke, N.C., Field, C., 2008. Threats to mangroves from climate change and adaptation options: a review. Aquat. Bot. 89 (2), 237–250. https://doi.org/10.1016/j.aquabot.2007.12.009.
Githumbi, E.N., 2017. Holocene Environmental and Human Interactions in East Africa. Unpublished PhD thesis, University of York, York.
Grimm, E.C., 1991. Tilia and Tiliagraph. Illinois State Museum, Springfield.
Grindrod, J., 1985. The palynology of mangroves on a prograded shore, princess charlotte bay, north queensland, Australia. J. Biogeogr. 12, 323–348. https://doi.org/10.2307/2844865.
Griffiths, M.L., Johnson, K.R., Pausata, F.S., White, J.C., Henderson, G.M., Wood, C.T., Yang, H., Ersek, V., Conrad, C., Sekhon, N., 2020. End of green sahara amplified mid- to late Holocene megadroughts in mainland Southeast Asia. Nat. Commun. 11 (1), 4204. https://doi.org/10.1038/s41467-020-17927-6.
Hammond, A.P., Goh, K.M., Tonkin, P.J., Manning, M.R., 1991. Chemical pretreatments for improving the radiocarbon dates of peats and organic silts in a gley podzol environment: grahams Terrace, North Westland. N. Z. J. Geol. Geophys. 34 (2), 191–194. https://doi.org/10.1080/00288306.1991.9514456.
Hawker, L., Uhe, P., Paulo, L., Sosa, J., Savage, J., Sampson, C., Neal, J., 2022. A 30 m global map of elevation with forests and buildings removed. Environ. Res. Lett. 17, 024016 https://doi.org/10.1088/1748-9326/ac4d4f.
Heiri, O., Lotter, A.F., Lemcke, G., 2001. Loss on ignition as a method for estimating organic and carbonate content in sediments: reproducibility and comparability of results. J. Paleolimnol. 25 (1), 101–110. https://doi.org/10.1023/A:1008119611481.
Hogarth, P.J., 2015. The Biology of Mangroves and Seagrasses. Oxford University Press.
Horton, B.P., Benjamin, P., Gibbard, L.G., Milne, M., Morley, R.J., Purintavaragul, C., Stargardt, J.M., 2005. Holocene sea levels and palaeoenvironments, Malay-Thai Peninsula, Southeast Asia. Holocene 15, 1199–1213. https://doi.org/10.1191/0959683605hl891rp.
Horton, B.P., Khan, N.S., Cahill, N., Lee, J.S., Shaw, T.A., Garner, A.J., Kemp, A.C., Engelhart, S.E., Rahmstorf, S., 2020. Estimating global mean sea-level rise and its uncertainties by 2100 and 2300 from an expert survey. Clim. and Atmo. Sci. 3 (1), 1–8. https://doi.org/10.1038/s41612-020-0121-5.
Kershaw, A.P., 1997. A modification of the Troels–Smith system of sediment description and portrayal. Quat. Australasia 15 (2), 63–68.
Krauss, K.W., Lovelock, C.E., McKee, K.L., Lopez-Hoffman, L., Ewe, S.M., Sousa, W.P., 2008. Environmental drivers in mangrove establishment and early development: a review. Aquat. Bot. 89 (2), 105–127. https://doi.org/10.1016/j.aquabot.2007.12.014.
Land Development Department, 2020. Landuse Data in Krabi Year 2020. Land Development Department, Ministry of Agriculture and Co-operatives, Bangkok.
Lieberman, V., Buckley, B., 2012. The impact of climate on Southeast Asia, circa 950–1820: new findings. Mod. Asian Stud. 46 (5), 1049–1096. https://doi.org/10.1017/S0026749X12000091.
Mann, T., Bender, M., Lorscheid, T., Stocchi, P., Vacchi, M., Switzer, A.D., Rovere, A., 2019. Holocene sea levels in southeast Asia, Maldives, India and Sri Lanka: the SEAMIS database. Quat. Sci. Rev. 219, 112–125. https://doi.org/10.1016/j.quascirev.2019.07.007.
Marchant, R., Hooghiemstra, H., 2004. Rapid environmental change in African and South American tropics around 4000 years before present: a review. Earth Sci. Rev. 66 (3–4), 217–260. https://doi.org/10.1016/j.earscirev.2004.01.003.
Maxwell, A.L., 2001. Holocene monsoon changes inferred from lake sediment pollen and carbonate records, northeastern Cambodia. Quat. Res. 56 (3), 390–400. https://doi.org/10.1006/qres.2001.2271.
Maxwell, A.L., 2004. Fire regimes in north-eastern Cambodian monsoonal forests, with a 9300-year sediment charcoal record. J. Biogeogr. 31 (2), 225–239. https://doi.org/10.1046/j.0305-0270.2003.01015.x.
Moraes, C.A., Fontes, N.A., Cohen, M.C., França, M.C., Pessenda, L.C., Rossetti, D.F., Francisquini, M.I., Bendassolli, J.A., Macario, K., 2017. Late Holocene mangrove dynamics dominated by autogenic processes. Earth Surf. Process. Landforms 42 (13), 2013–2023. https://doi.org/10.1002/esp.4167.
Nace, T.E., Baker, P.A., Dwyer, G.S., Silva, C.G., Rigsby, C.A., Burns, S.J., Giosan, L., Otto-Bliesner, B., Liu, Z., Zhu, J., 2014. The role of North Brazil Current transport in the paleoclimate of the Brazilian Nordeste margin and paleoceanography of the western tropical Atlantic during the late Quaternary. Palaeogeogr. Palaeoclimatol. Palaeoecol. 415, 3–13. https://doi.org/10.1016/j.palaeo.2014.05.030.
Newnham, R.M., Vandergoes, M.J., Garnett, M.H., Lowe, D.J., Prior, C., Almond, P.C., 2007. Test of AMS 14C dating of pollen concentrates using tephrochronology. J. Quat. Sci. 22 (1), 37–51. https://doi.org/10.1002/jqs.101.
Oliver, G.J.H., Terry, J.P., 2019. Relative sea-level highstands in Thailand since the Mid-Holocene based on 14C rock oyster chronology. Palaeogeogr. Palaeoclimatol. Palaeoecol. 517, 30–38. https://doi.org/10.1016/j.palaeo.2018.12.005.
Peltier, W.R., Argus, D.F., Drummond, R., 2015. Space geodesy constrains ice age terminal deglaciation: the global ICE- 6G_C (VM5a) model. J. Geophys. Res. Solid Earth 120, 450–487. https://doi.org/10.1002/2014JB011176.
Phengklai, C., 1981. Elaeocarpaceae. In: Phengklai, C. (Ed.), Flora of Thailand 2 (4). The Forest Herbarium, Bangkok, pp. 405–438.

Pramojanee, P., Hastings, P., Liengsakul, M., Engakul, V., 1986. The Holocene transgression in peninsular Thailand. Geol. Soc. Malays. Bull. 19, 551–564.
Punwong, P., Marchant, R., Selby, K., 2012. Holocene mangrove dynamics and environmental change in the Rufiji Delta, Tanzania. Veg. Hist. Archaeobotany 21 (6), 1–16. https://doi.org/10.1007/s00334-012-0383-x.
Punwong, P., Marchant, R., Selby, K., 2013a. Holocene mangrove dynamics from unguja ukuu, zanzibar. Quat. Int. 298, 4–19. https://doi.org/10.1016/j.quaint.2013.02.007.
Punwong, P., Marchant, R., Selby, K., 2013b. Holocene mangrove dynamics and sea level changes in Makoba Bay. Zanzibar Palaeogeogr, Palaeoclimatol., Palaeoecol. 379–380, 54–67. https://doi.org/10.1016/j.ecss.2018.07.004.
Punwong, P., Sritrairat, S., Selby, K., Marchant, R., Pumijumnong, N., Traiperm, P., 2018. An 800 year record of mangrove dynamics and human activities in the upper Gulf of Thailand. Veg. Hist. Archaeobotany 27 (4), 535–549. https://doi.org/10.1007/s00334-017-0651-x.
Punwong, P., Englong, A., Traiperm, P., Chabangborn, A., 2021. Vegetation history and human impacts from Thong Pha Phum, western Thailand during the past 700 years. Veg. Hist. Archaeobotany 30, 383–394. https://doi.org/10.1007/s00334-020-00786-y.
Punwong, P., Promplin, S., Lomchantrasilp, C., Soonthornampaipong, P., Englong, A., Marchant, R., Selby, K., Chirawatkul, P., 2023. Documenting a thousand years of environmental and anthropogenic changes on mangroves on the Bangkok coast, the upper Gulf of Thailand. Veg. Hist. Archaeobotany 32 (1), 17–34. https://doi.org/10.1007/s00334-022-00876-z.
Putcharapitchakon, K., Ritphring, S., 2012. Sea level change in Thailand. Ladkrabang Eng. J. 29 (3), 55–60 (in Thai).
Reimer, P.J., Austin, W.E., Bard, E., Bayliss, A., Blackwell, P.G., Ramsey, C.B., Butzin, M., Cheng, H., Edwards, R.L., Friedrich, M., Grootes, P.M., 2020. The IntCal20 Northern Hemisphere radiocarbon age calibration curve (0–55 cal kBP). Radiocarbon 62 (4), 725–757. https://doi.org/10.1017/RDC.2020.41.
Ribeiro, S.R., Batista, E.J.L., Cohen, M.C., França, M.C., Pessenda, L.C., Fontes, N.A., Alves, I.C., Bendassolli, J.A., 2018. Allogenic and autogenic effects on mangrove dynamics from the Ceará Mirim River, north-eastern Brazil, during the middle and late Holocene. Earth Surf. Process. Landforms 43 (8), 1622–1635. https://doi.org/10.1002/esp.4342.
Rucina, S.M., Muiruri, V.M., Downton, L., Marchant, R., 2010. Late Holocene savanna dynamics in the amboseli basin, Kenya. Holocene 20 (5), 667–677. https://doi.org/10.1177/0959683609358910.
Somsak, R., Jantakham, S., 2013. Geological Map of Changwat Krabi. Department of Mineral Resources, Bangkok.
Santisuk, T., 1983. Taxonomy and distribution of terrestrial trees and shrubs in the mangrove formations in Thailand. Nat. Hist. Bull. Siam Soc. 5 (1), 63–91.
Sarkar, A., Ramesh, R., Somayajulu, B.L.K., Agnihotri, R., Jull, A.J.T., Burr, G.S., 2000. High resolution Holocene monsoon record from the eastern Arabian Sea. Earth Planet Sci. Lett. 177, 209–218. https://doi.org/10.1016/S0012-821X(00)00053-4.
Scheffers, A., Brill, D., D, Kelletat, H. Brückner, Scheffers, S., Fox, K., 2012. Holocene sea levels along the Andaman Sea coast of Thailand. Holocene 22, 1169–1180. https://doi.org/10.1177/0959683612441803.
Scoffin, T.P., Tissier, M.D.A.L., 1998. Late Holocene sea level and reef-flat progradation, Phuket, South Thailand. Coral Reefs 17, 273–276. https://doi.org/10.1007/s003380050128.
Solé, V.A., Papillon, E., Cotte, M., Walter, P., Susini, J.A., 2007. A multiplat- form code for the analysis of energy-dispersive X-ray fluorescence spectra. Spectrochim. Acta, Part B 62, 63–68. https://doi.org/10.1016/j.sab.2006.12.002.
Tam, C.Y., Zong, Y., bin Hassan, K., bin Ismal, H., binti Jamil, H., Xiong, H., Wu, P., Sun, Y., Huang, G., Zheng, Z., 2018. A below-the-present late Holocene relative sea level and the glacial isostatic adjustment during the Holocene in the Malay Peninsula. Quat. Sci. Rev. 201, 206–222. https://doi.org/10.1016/j.quascirev.2018.10.009.
Tjia, H.D., 1996. Sea-level changes in the tectonically stable Malay-Thai Peninsula. Quat. Int. 31, 95–101. https://doi.org/10.1016/1040-6182(95)00025-E.
Toscano, M.A., Macintyre, I.G., 2003. Corrected western Atlantic sea-level curve for the last 11,000 years based on calibrated $^{14}$C dates from Acropora palmata framework and intertidal mangrove peat. Coral Reefs 22, 257–270. https://doi.org/10.1007/s00338-003-0315-4.
Uhe, P., Hawker, L., Paulo, L., Sosa, J., Sampson, C., Neal, J., 2022. FABDEM - A 30m Global Map of Elevation with Forests and Buildings Removed. EGU General Assembly 2022, Vienna, Austria, 23–27 May 2022, EGU22-8994.
Wang, Y.S., Gu, J.D., 2021. Ecological responses, adaptation and mechanisms of mangrove wetland ecosystem to global climate change and anthropogenic activities. Int. Biodeterior. Biodegrad. 162, 105248 https://doi.org/10.1016/j.ibiod.2021.105248.
Watson, J.G., 1928. Mangrove forests of the Malay Peninsula. Malay. For. Rec. 6, 275.
Whitlock, C., Larsen, C., 2001. Charcoal as a fire proxy. In: Smol, J.P., Birks, H.J.B., Last, W.M. (Eds.), Tracking Environmental Change Using Lake Sediments: Volume 3: Terr., Algal, and Siliceous Indic, vol. 3, p. 75.
Wohlfarth, B., Higham, C., Yamoah, K.A., Chabangborn, A., Chawchai, S., Smittenberg, R.H., 2016. Human adaptation to mid-to late- Holocene climate change in Northeast Thailand. Holocene 26, 1875–1886. https://doi.org/10.1177/0959683616645947.
Woodroffe, S.A., 2009. Testing models of mid-late Holocene sea-level change, North Queensland, Australia. Quat. Sci. Rev. 28, 2474–2488. https://doi.org/10.1016/j.quascirev.2009.05.004.
Woodroffe, S.A., Horton, B.P., 2005. Holocene sea-level changes in the Indo-Pacific. J. Asian Earth Sci. 25, 29–43. https://doi.org/10.1016/j.jseaes.2004.01.009.
Yamoah, K.A., Higham, C.F., Wohlfarth, B., Chabangborn, A., Chawchai, S., Schenk, F., Smittenberg, R.H., 2017. Societal response to monsoonal fluctuations in NE Thailand during the demise of Angkor Civilisation. Holocene 27 (10), 1455–1464. https://doi.org/10.1177/0959683617693900.